Supplemental Information for:

NF-κB activating complex engaged in response to EGFR oncogene inhibition drives tumor cell survival and residual disease in lung cancer

Authors: Collin M. Blakely, Evangelos Pazarentzos, Victor Olivas, Saurabh Asthana, Jenny Jiacheng Yan, Irena Tan, Gorjan Hrustanovic, Elton Chan, Luping Lin, Dana S. Neel, William Newton, Kathryn Bobb,Timothy Fouts, Jeffrey Meshulam, Matthew A. Gubens, David M. Jablons, Jeffrey Johnson, Sourav Bandyopadhyay, Nevan Krogan, and Trever G. Bivona

This PDF includes:

Supplemental Figures:

Supplemental Tables:

Supplemental Experimental Procedures:

Supplemental References

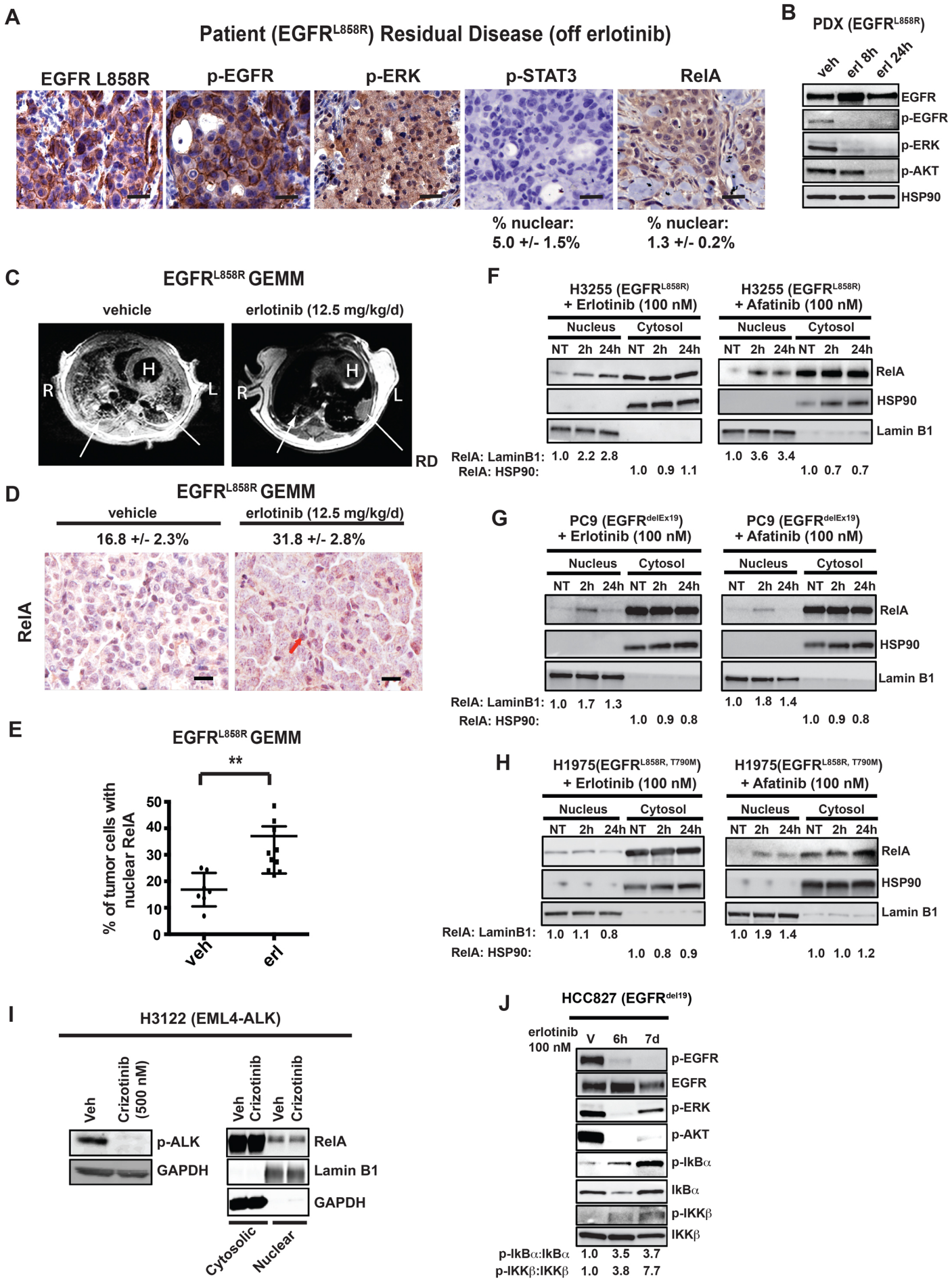
A
Patient (EGFR L858R) Residual Disease (off erlotinib)
EGFR L858R
p-EGFR
p-ERK
p-STAT3
RelA
% nuclear:
5.0 +/- 1.5%
% nuclear:
1.3 +/- 0.2%
B
PDX (EGFR L858R)
veh
erl 8h
erl 24h
EGFR
p-EGFR
p-ERK
p-AKT
HSP90
C
EGFR L858R GEMM
vehicle
erlotinib (12.5 mg/kg/d)
H
R
L
RD
D
EGFR L858R GEMM
vehicle
erlotinib (12.5 mg/kg/d)
16.8 +/- 2.3%
31.8 +/- 2.8%
RelA
E
EGFR L858R GEMM
**
% of tumor cells with nuclear RelA
50
40
30
20
10
0
veh
erl
F
H3255 (EGFR L858R)
+ Erlotinib (100 nM)
H3255 (EGFR L858R)
+ Afatinib (100 nM)
Nucleus
Cytosol
NT 2h 24h NT 2h 24h
RelA
HSP90
Lamin B1
RelA: LaminB1: 1.0 2.2 2.8
RelA: HSP90: 1.0 0.9 1.1
1.0 3.6 3.4
1.0 0.7 0.7
G
PC9 (EGFR delEx19)
+ Erlotinib (100 nM)
PC9 (EGFR delEx19)
+ Afatinib (100 nM)
RelA: LaminB1: 1.0 1.7 1.3
RelA: HSP90: 1.0 0.9 0.8
1.0 1.8 1.4
1.0 0.9 0.8
H
H1975(EGFR L858R, T790M)
+ Erlotinib (100 nM)
H1975(EGFR L858R, T790M)
+ Afatinib (100 nM)
RelA: LaminB1: 1.0 1.1 0.8
RelA: HSP90: 1.0 0.8 0.9
1.0 1.9 1.4
1.0 1.0 1.2
I
H3122 (EML4-ALK)
Veh
Crizotinib (500 nM)
p-ALK
GAPDH
Veh
Crizotinib
Veh
Crizotinib
RelA
Lamin B1
GAPDH
Cytosolic
Nuclear
J
HCC827 (EGFR del19)
erlotinib 100 nM
V
6h
7d
p-EGFR
EGFR
p-ERK
p-AKT
p-IkBα
IkBα
p-IKKβ
IKKβ
p-IkBα:IkBα 1.0 3.5 3.7
p-IKKβ:IKKβ 1.0 3.8 7.7

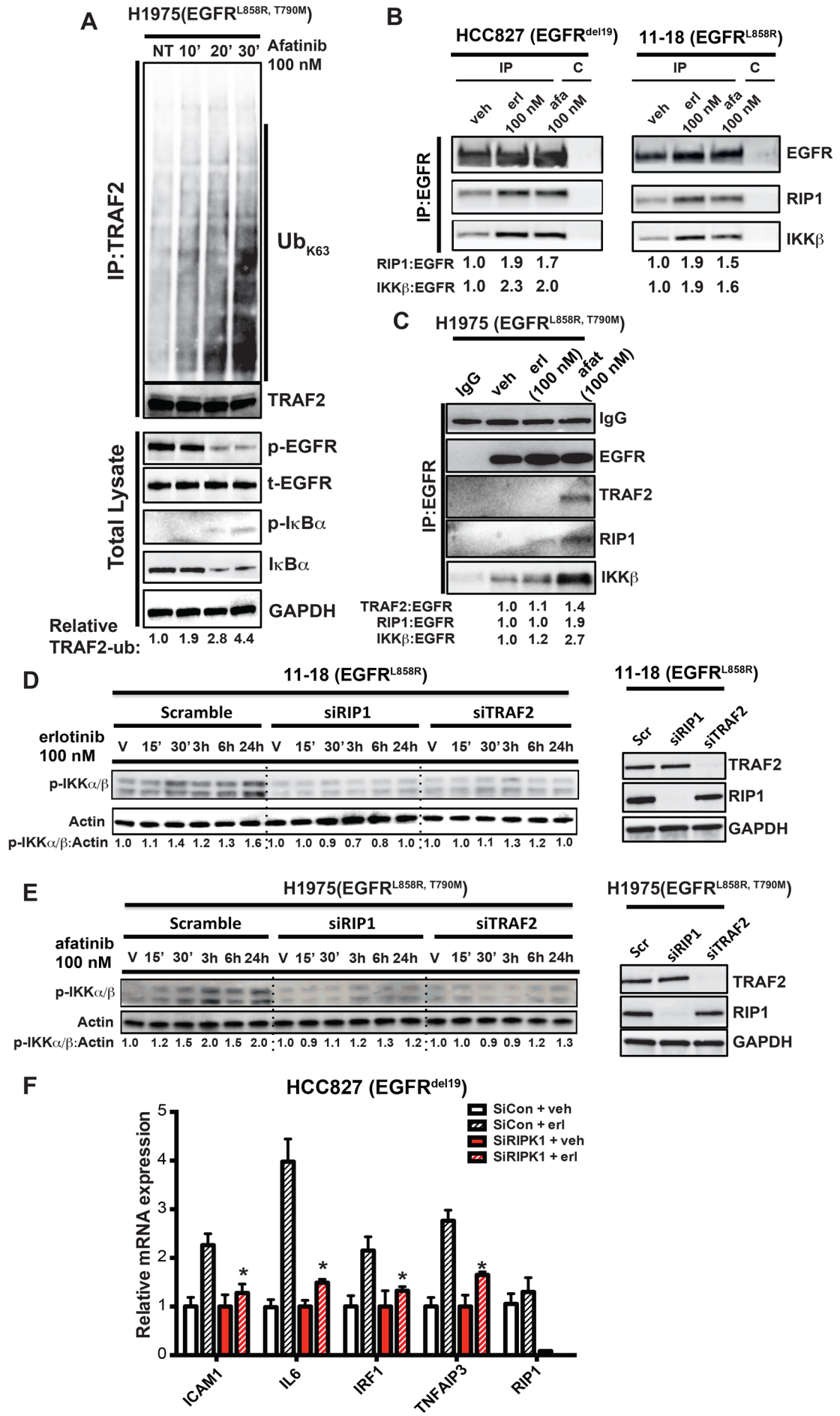
A
H1975(EGFR L858R, T790M)
NT 10' 20' 30'
Afatinib 100 nM
IP:TRAF2
Ub K63
TRAF2
Total Lysate
p-EGFR
t-EGFR
p-IκBα
IκBα
GAPDH
Relative TRAF2-ub: 1.0 1.9 2.8 4.4
B
HCC827 (EGFR del19)
11-18 (EGFR L858R)
IP
C
veh
erl 100 nM
afa 100 nM
IP:EGFR
EGFR
RIP1
IKKβ
RIP1:EGFR 1.0 1.9 1.7
IKKβ:EGFR 1.0 2.3 2.0
1.0 1.9 1.5
1.0 1.9 1.6
C
H1975 (EGFR L858R, T790M)
IgG
veh
erl (100 nM)
afat (100 nM)
IP:EGFR
IgG
EGFR
TRAF2
RIP1
IKKβ
TRAF2:EGFR 1.0 1.1 1.4
RIP1:EGFR 1.0 1.0 1.9
IKKβ:EGFR 1.0 1.2 2.7
D
11-18 (EGFR L858R)
Scramble
siRIP1
siTRAF2
erlotinib 100 nM
V 15' 30' 3h 6h 24h V 15' 30' 3h 6h 24h V 15' 30' 3h 6h 24h
p-IKKα/β
Actin
p-IKKα/β:Actin 1.0 1.1 1.4 1.2 1.3 1.6 1.0 1.0 0.9 0.7 0.8 1.0 1.0 1.0 1.1 1.3 1.2 1.0
11-18 (EGFR L858R)
Scr
siRIP1
siTRAF2
TRAF2
RIP1
GAPDH
E
H1975(EGFR L858R, T790M)
Scramble
siRIP1
siTRAF2
afatinib 100 nM
V 15' 30' 3h 6h 24h V 15' 30' 3h 6h 24h V 15' 30' 3h 6h 24h
p-IKKα/β
Actin
p-IKKα/β:Actin 1.0 1.2 1.5 2.0 1.5 2.0 1.0 0.9 1.1 1.2 1.3 1.2 1.0 1.0 0.9 0.9 1.2 1.3
H1975(EGFR L858R, T790M)
Scr
siRIP1
siTRAF2
TRAF2
RIP1
GAPDH
F
HCC827 (EGFR del19)
SiCon + veh
SiCon + erl
SiRIPK1 + veh
SiRIPK1 + erl
Relative mRNA expression
0
1
2
3
4
5
*
ICAM1
IL6
IRF1
TNFAIP3
RIP1

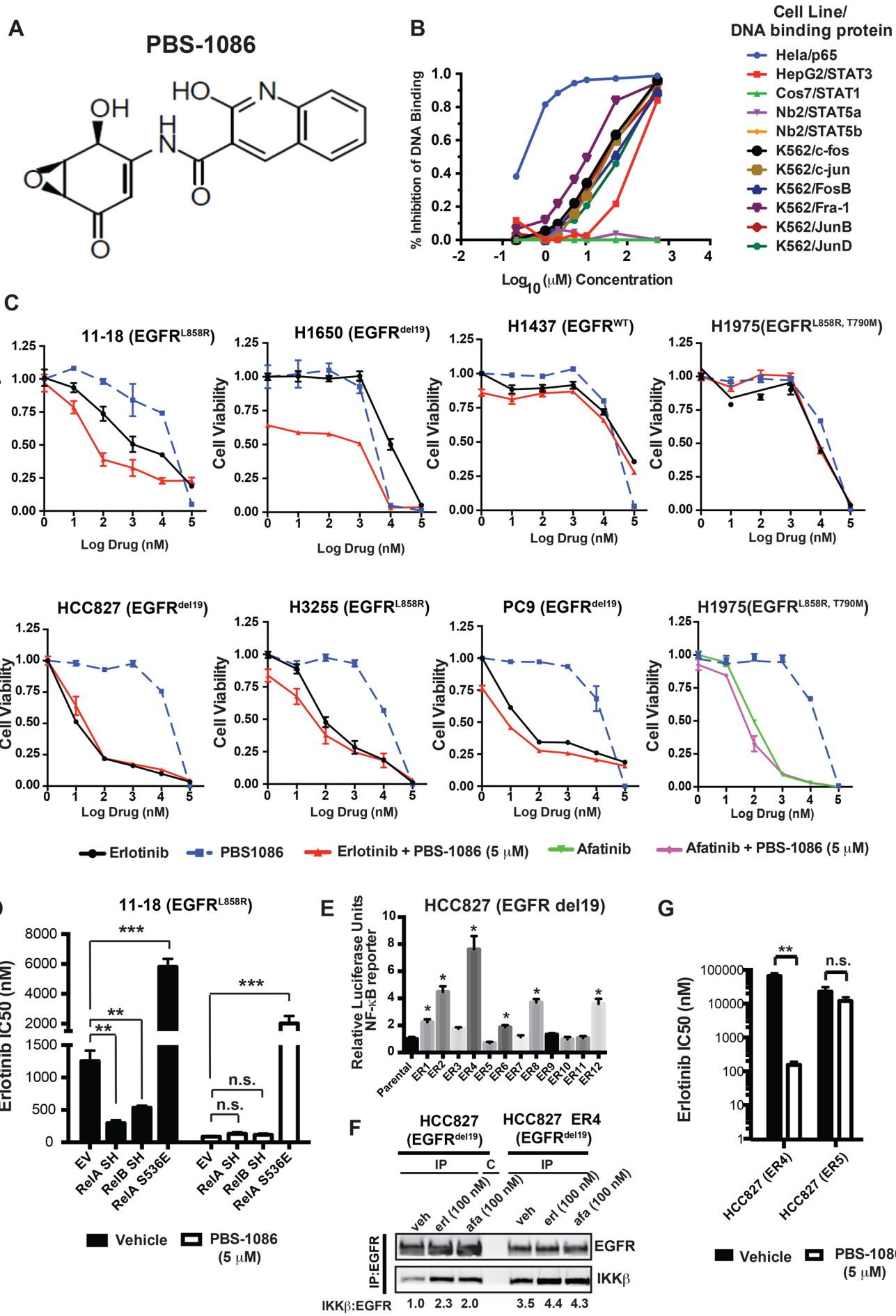
A
PBS-1086
OH
HO
N
H
N
O
O
O
B
Cell Line/
DNA binding protein
Hela/p65
HepG2/STAT3
Cos7/STAT1
Nb2/STAT5a
Nb2/STAT5b
K562/c-fos
K562/c-jun
K562/FosB
K562/Fra-1
K562/JunB
K562/JunD
% Inhibition of DNA Binding
Log10 (μM) Concentration
C
11-18 (EGFRL858R)
H1650 (EGFRdel19)
H1437 (EGFRWT)
H1975(EGFRL858R, T790M)
HCC827 (EGFRdel19)
H3255 (EGFRL858R)
PC9 (EGFRdel19)
H1975(EGFRL858R, T790M)
Cell Viability
Log Drug (nM)
Erlotinib
PBS1086
Erlotinib + PBS-1086 (5 μM)
Afatinib
Afatinib + PBS-1086 (5 μM)
D
11-18 (EGFRL858R)
Erlotinib IC50 (nM)
EV
RelA SH
RelB SH
RelA S536E
n.s.
Vehicle
PBS-1086
(5 μM)
E
HCC827 (EGFR del19)
Relative Luciferase Units
NF-κB reporter
Parental
ER1
ER2
ER3
ER4
ER5
ER6
ER7
ER8
ER9
ER10
ER11
ER12
F
HCC827
(EGFRdel19)
HCC827 ER4
(EGFRdel19)
IP
C
veh
erl (100 nM)
afa (100 nM)
IP:EGFR
EGFR
IKKβ
IKKβ:EGFR
1.0 2.3 2.0
3.5 4.4 4.3
G
Erlotinib IC50 (nM)
n.s.
HCC827 (ER4)
HCC827 (ER5)
Vehicle
PBS-1086
(5 μM)

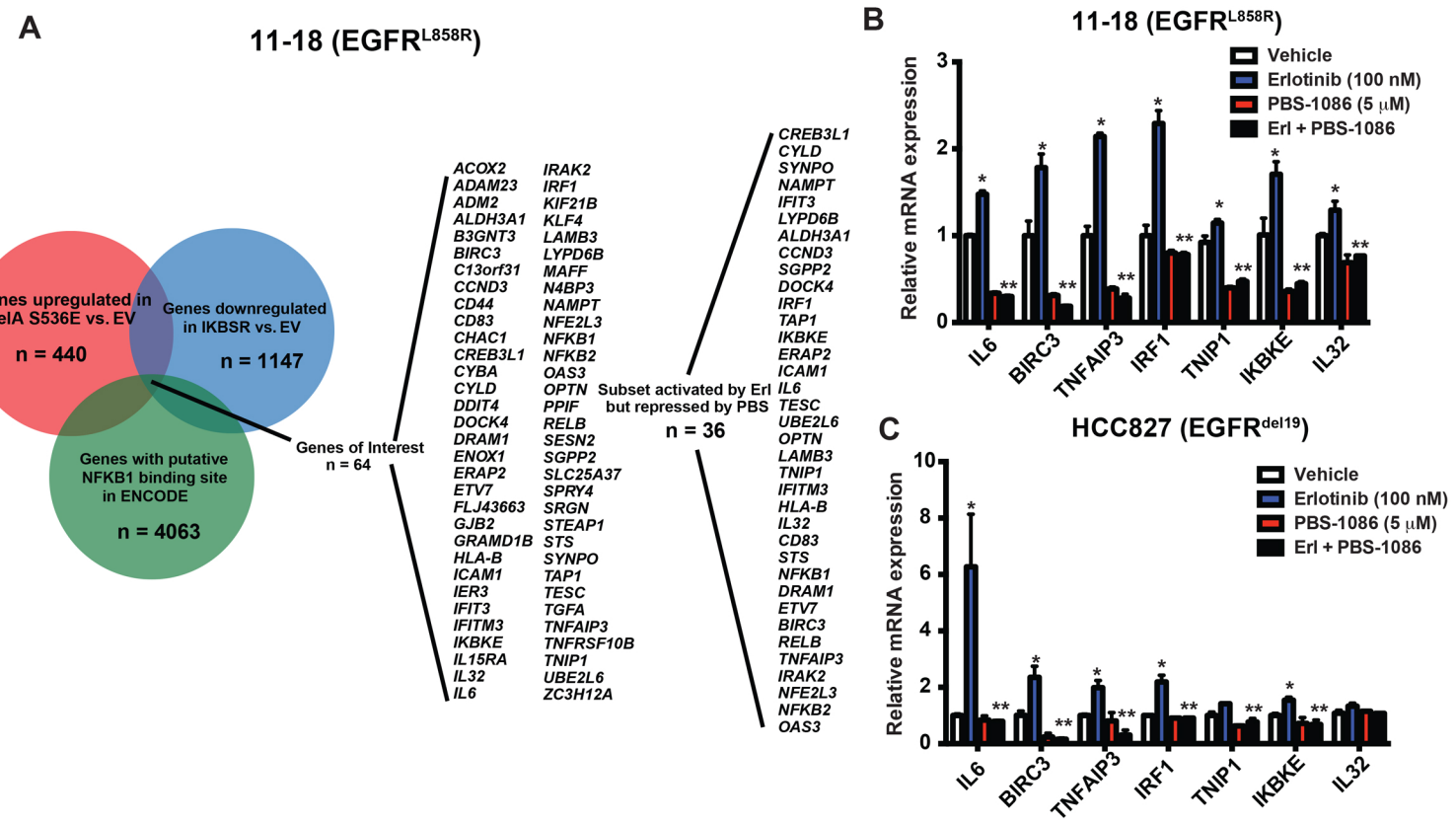
A
11-18 (EGFR L858R)
Genes upregulated in RelA S536E vs. EV
n = 440
Genes downregulated in IKBSR vs. EV
n = 1147
Genes with putative NFKB1 binding site in ENCODE
n = 4063
Genes of Interest
n = 64
ACOX2 ADAM23 ADM2 ALDH3A1 B3GNT3 BIRC3 C13orf31 CCND3 CD44 CD83 CHAC1 CREB3L1 CYBA CYLD DDIT4 DOCK4 DRAM1 ENOX1 ERAP2 ETV7 FLJ43663 GJB2 GRAMD1B HLA-B ICAM1 IER3 IFIT3 IFITM3 IKBKE IL15RA IL32 IL6
IRAK2 IRF1 KIF21B KLF4 LAMB3 LYPD6B MAFF N4BP3 NAMPT NFE2L3 NFKB1 NFKB2 OAS3 OPTN PPIF RELB SESN2 SGPP2 SLC25A37 SPRY4 SRGN STEAP1 STS SYNPO TAP1 TESC TGFA TNFAIP3 TNFRSF10B TNIP1 UBE2L6 ZC3H12A
Subset activated by Erl but repressed by PBS
n = 36
CREB3L1 CYLD SYNPO NAMPT IFIT3 LYPD6B ALDH3A1 CCND3 SGPP2 DOCK4 IRF1 TAP1 IKBKE ERAP2 ICAM1 IL6 TESC UBE2L6 OPTN LAMB3 TNIP1 IFITM3 HLA-B IL32 CD83 STS NFKB1 DRAM1 ETV7 BIRC3 RELB TNFAIP3 IRAK2 NFE2L3 NFKB2 OAS3
B
11-18 (EGFR L858R)
Vehicle
Erlotinib (100 nM)
PBS-1086 (5 μM)
Erl + PBS-1086
Relative mRNA expression
IL6 BIRC3 TNFAIP3 IRF1 TNIP1 IKBKE IL32
C
HCC827 (EGFR del19)
Vehicle
Erlotinib (100 nM)
PBS-1086 (5 μM)
Erl + PBS-1086
Relative mRNA expression
IL6 BIRC3 TNFAIP3 IRF1 TNIP1 IKBKE IL32

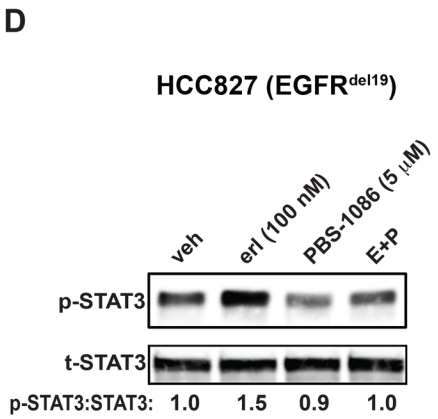
D
HCC827 (EGFR del19)
veh
erl (100 nM)
PBS-1086 (5 μM)
E+P
p-STAT3
t-STAT3
p-STAT3:STAT3: 1.0 1.5 0.9 1.0

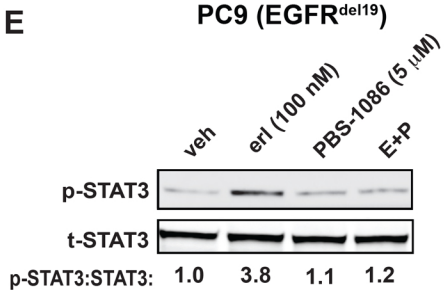
E
PC9 (EGFR del19)
veh
erl (100 nM)
PBS-1086 (5 μM)
E+P
p-STAT3
t-STAT3
p-STAT3:STAT3: 1.0 3.8 1.1 1.2

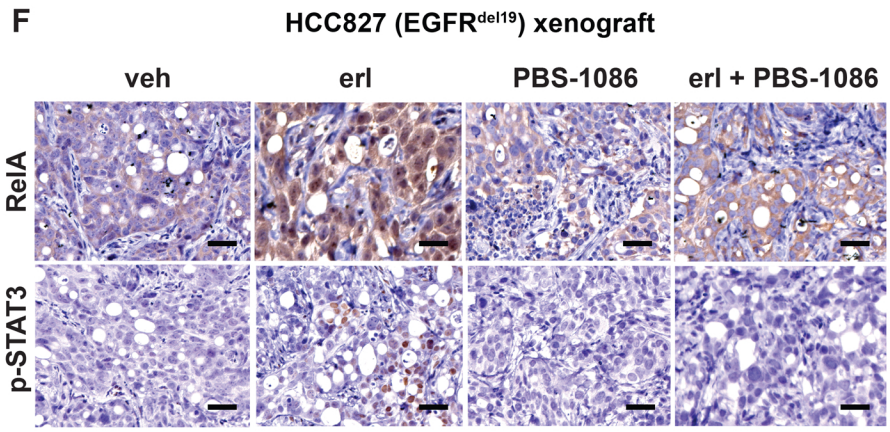
F
HCC827 (EGFR del19) xenograft
veh
erl
PBS-1086
erl + PBS-1086
RelA
p-STAT3

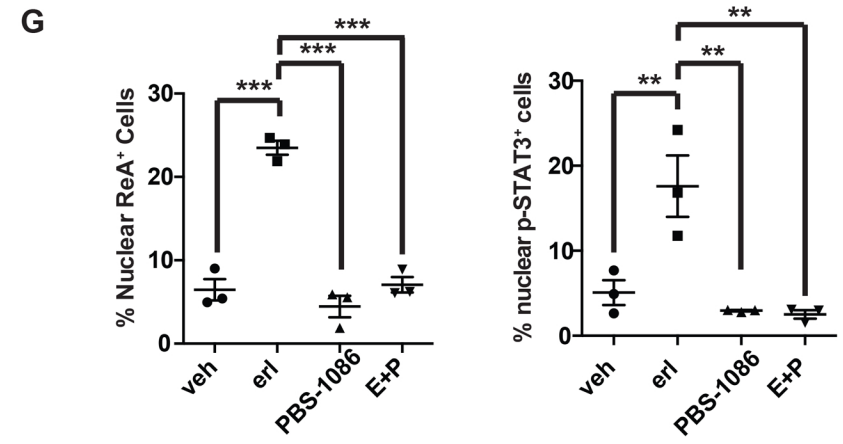
G
% Nuclear ReA+ Cells
% nuclear p-STAT3+ cells
veh
erl
PBS-1086
E+P

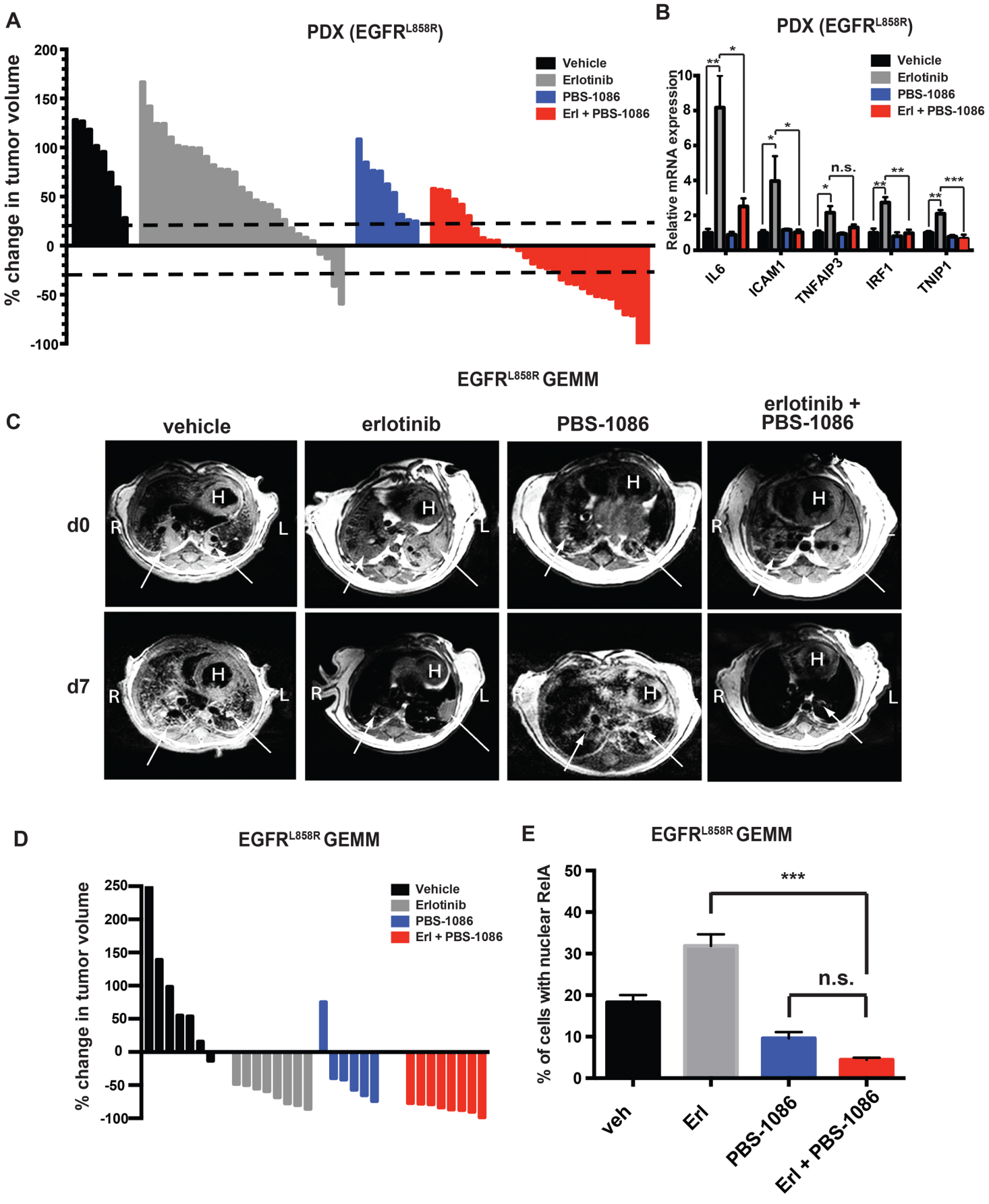
A
PDX (EGFR^{L858R})
% change in tumor volume
200
150
100
50
0
-50
-100
Vehicle
Erlotinib
PBS-1086
Erl + PBS-1086
B
PDX (EGFR^{L858R})
Relative mRNA expression
10
8
6
4
2
0
Vehicle
Erlotinib
PBS-1086
Erl + PBS-1086
**
*
*
*
*
n.s.
**
**
**
***
IL6
ICAM1
TNFAIP3
IRF1
TNIP1
EGFR^{L858R} GEMM
C
vehicle
erlotinib
PBS-1086
erlotinib + PBS-1086
d0
d7
H
R
L
D
EGFR^{L858R} GEMM
% change in tumor volume
250
200
150
100
50
0
-50
-100
Vehicle
Erlotinib
PBS-1086
Erl + PBS-1086
E
EGFR^{L858R} GEMM
% of cells with nuclear RelA
50
40
30
20
10
0
***
n.s.
veh
Erl
PBS-1086
Erl + PBS-1086

Table S1

Transcription Factor	**PBS-1086 IC50 (μM)**
P65 (RelA)	0.3
STAT1	5.3
STAT5b	5.3
Fra-1	9.9
JunB	32.8
c-fos	48.1
c-jun	49.9
STAT3	97.1
FosB	107.9
JunD	177.4
STAT5a	ND

Table S2. Effect of PBS-1086 on transcription factor gene set expression.

Gene Set	NES	p-value
GGGNNTTTCC_NFKB Q6 01	-1.77	0.044
CREL_01	-1.57	0.081
NFKB_Q6_01	-1.52	0.047
MYCMAX	-0.95	0.375
AP1_Q4	-0.94	0.383
E2F_Q6_01	-0.81	0.77
NFAT_Q4_01	-0.61	0.99

Table S3. Response of EGFR-L858R PDX tumors to erlotinib and PBS-1086.

Response	Erlotinib	Erlotinib + PBS-1086	P-Value
ORR (PR + CR)	6.9%	42.0%	0.002
DCR (SD + PR + CR)	27.5%	80.6%	< 0.001
PR	6.9%	35.5%	0.011
CR	0.0%	6.4%	0.49
PD	72.5%	19.4%	<0.001

ORR: Objective Response Rate
DCR: Disease Control Rate
PR: Partial Response (> 30 % decrease in tumor size)
CR: Complete Response (100 % decrease in tumor size).
PD: Progressive Disease (> 20% increase in tumor size).

Supplemental Figure and Table Legends.

Figure S1. Induction of NF-κB upon EGFR TKI treatment in NSCLC, related to Figure 1. (A) Representative IHC staining for the indicated proteins performed on residual EGFR L858R-mutant NSCLC resected from patient. Scale bar = 50 microns. Quantitation of nuclear p-STAT3 and RelA (mean ± S.E.M) is indicated **(B)** Western blot showing the effects of erlotinib treatment of PDX tumors on the phosphorylation of the indicated proteins. **(C)** Representative Magnetic resonance imaging (MRI) of CC10-rtTA;TetO-EGFR^{L858R} transgenic mice (EGFR^{L858R} GEMM) treated with doxycycline for 10 weeks (d0) to induce lung adenocarcinoma formation, followed by treatment with vehicle or erlotinib (12.5 mg/kg/d) for 7 days. H indicates the position of the heart. White arrows indicate the position of lung tumors. Residual disease after erlotinib treatment is indicated (RD). **(D-E)** IHC staining and quantitation of nuclear RelA in CC10-rtTA; TetO-EGFR^{L858R} transgenic mouse tumors following treatment with vehicle or erlotinib (mean ± S.E.M.). ** $p < 0.01$.

(F-H) Western blots showing the effect of erlotinib and afatinib on nuclear localization of RelA in the indicated EGFR-mutant NSCLC cell lines. **(I)** Western blots showing the effect of crizotinib on ALK phosphorylation and nuclear localization of RelA in the EML4-ALK positive NSCLC cell line H3122. **(J)** Western blot of HCC827 cells treated as indicated for 6h or 7 days. Live cells attached to the culture plate were harvested for analysis.

Figure S2. Induction of NF-κB activating complex upon EGFR TKI treatment of NSCLC cells, related to Figure 2. (A) TRAF2 immunoprecipitation and K63 ubiquitination in H1975 cells transfected with HA-Ubiquitin K63 plasmid and treated

with afatinib (100 nM) for the indicated periods of time. **(B-C)** Immunoprecipitation of endogenous EGFR from HCC827, 11-18 (B), and H1975 (C) cells treated with erlotinib or afatinib as indicated, showing the assembly of the NF-κB signaling complex. **(D-E)** Western blot analysis of EGFR and NF-κB signaling in 11-18 **(D)** and H1975 **(E)** cells treated with RIP1 and TRAF2 specific siRNAs ± erlotinib or afatinib. In each case, the phosphorylation of the NF-κB activating kinase IKKa/b was used as a biomarker for upstream activation of NF-κB signaling, revealing attenuation of EGFR TKI-induced p-IKKa/b upon either RIP1 or TRAF2 knockdown compared to cells with the scrambled control siRNA. **(F)** Q-PCR demonstrating mRNA expression of selected NF-κB target genes in response to erlotinib treatment of HCC827 cells transfected with the indicated siRNAs (mean ± S.E.M.). * $p < 0.05$ compared to erlotinib treated SiControl as determined by by two-tailed unpaired T-test.

Figure S3. Effects of pharmacologic direct NF-κB inhibitor in NSCLC, related to Figure 3. (A) Chemical structure of PBS-1086. **(B)** In vitro DNA binding assay of indicated transcription factors upon treatment of nuclear extracts with the indicated concentration of PBS-1086. **(C)** Cell viability assays of the indicated lung adenocarcinoma cell lines treated with increasing concentrations of erlotinib or afatinib or PBS-1086, or a combination of erlotinib + PBS-1086 or afatinib + PBS-1086. Cell viability was assessed 72 hours after the start of treatment and is plotted for each drug concentration (mean ± S.E.M.). **(D)** Drug sensitivity as measured by half maximal inhibitory concentration (IC_{50}) of erlotinib (mean ± S.E.M.) in 11-18 cells transfected with expression vectors to stably express a RelA ShRNA, RelB ShRNA, or constitutively active RelA (S536E) compared to empty-vector transfected cells (EV). ** $p < 0.01$, ***

$p < 0.001$ as determined by Bonferroni's multiple comparisons ANOVA test. **(E)** Relative luciferase units (mean ± S.E.M.) in each of 12 erlotinib resistant (ER) HCC827 cell lines that had been transfected with an NF-κB luciferase reporter prior to erlotinib exposure. * $p < 0.05$ compared to luciferase activity in HCC827 parental lines by two-tailed unpaired T-test. **(F)** HCC827 parental cells and HCC827 ER4 cells were treated with vehicle, erlotinib, or afatinib and immunoprecipitation of EGFR was performed after 6 hours of treatment. Western blots were performed showing the assembly of the NF-κB signalosome upon EGFR inhibition in each of the cell lines. **(G)** Drug sensitivity as measured by half maximal inhibitory concentration (IC_{50}) of erlotinib (mean ± S.E.M.) in indicated cell lines treated with vehicle or PBS-1086. ** $p < 0.01$ compared to vehicle treated cells as determined by two-tailed unpaired T-test.

Figure S4. Identification of the transcriptional survival program induced by NF-κB activation that is triggered in response to EGFR oncogene inhibition, related to Figure 4. (A) Venn diagram demonstrating how the signature of NF-κB regulated gene expression changes was developed using genetic activation or silencing of NF-κB, in conjunction with the ENCODE dataset identifying genes with direct NF-κB binding sites. **(B-C)** Effect of PBS-1086 treatment on erlotinib-induced NF-κB target gene activation in **(B)** 11-18 and **(C)** HCC827 cells by Q-PCR (mean ± S.E.M.). * $P < 0.05$ compared to vehicle treatment, ** $p < 0.01$ compared to erlotinib treatment alone by Bonferroni's multiple comparisons ANOVA test. **(D-E)** Western blots demonstrating relative expression of p-STAT3 and total STAT3 in HCC827 and PC9 cells treated as indicated for 6 hours. **(F-G)** IHC analysis and quantitation for nuclear RelA and p-STAT3 expression in HCC827 tumor xenografts treated as indicated for 48 hours.

Figure S5. Effects of the direct pharmacologic NF-κB inhibitor PBS-1086 on residual disease and response *in vivo* in NSCLC, related to Figure 5. **(A)** Change in tumor volume of individual EGFR-mutant NSCLC patient-derived xenografts over a 10-day period of treatment of mice with the drugs indicated. **(B)** Quantitative real-time PCR (Q-PCR) analysis of indicated NF-κB target gene expression performed on RNA extracted from PDX tumors harvested from mice treated as indicated for 48 hours (mean ± S.E.M.). * $p < 0.05$, ** $p < 0.01$, *** $p < 0.001$ as determined by Bonferroni's multiple comparisons ANOVA test. **(C)** Magnetic resonance imaging (MRI) of $EGFR^{L858R}$ GEMM mice treated with doxycycline for 10 weeks (d0) followed by treatment with the indicated drugs for 7 days (d7). Images are representative of a minimum of 3 mice per treatment group. **(D)** Quantitation of individual lung tumor volume changes (determined by MRI) in $EGFR^{L858R}$ GEMM (CC10-rtTA; TetO-$EGFR^{L858R}$) mice treated with the indicated drug combinations for 7 days. **(E)** Quantitation of nuclear RelA IHC performed on lung tumors from $EGFR^{L858R}$ GEMM mice treated with the indicated drug combinations for 7 days (mean ± S.E.M.). *** $p < 0.001$ compared to erlotinib treatment alone by Bonferroni's multiple comparisons ANOVA test.

Table S1: Effects of PBS-1086 on DNA binding by RelA and selected transcription factors, related to Figure 3. Half-maximal inhibitory concentration of PBS-1086 against DNA binding by the transcription factors shown in nuclear extracts, showing selectivity for inhibition of RelA DNA binding. **ND = none detected.**

Table S2: Effects of PBS-1086 on transcription factor gene set expression. Related to Figure 3. Gene set enrichment analysis (GSEA) performed on RNA-Seq data obtained upon treating 11-18 cells with vehicle or PBS-1086. NES is Negative Enrichment Score.

Table S3: Response of EGFR-L858R PDX tumor to erlotinib and PBS-1086. Related to Figure 5. Comparison of PDX tumor response rates to the indicated drug treatments. P-Value determined by Fischer's Exact test.

Supplemental Experimental Procedures.

Cell lines and Reagents

Cells were grown in RPMI 1640 supplemented with 10% fetal bovine serum (FBS), penicillin G (100U/ml) and streptomycin SO_4 (100U/ml). Drugs were resuspended in DMSO at a concentration of 10 mM and stored at -20 °C. Erlotinib, afatinib, and PBS-1086 were used at working concentrations ranging from 0.01-10 micromolar. Ruxolitinib and imatinib were used at working concentrations of 1.0 micromolar. siRNA smartpools specific for *RIP1*, *TRAF2*, *IL6*, or scramble control were purchased from Thermo Scientific and used per manufacturer's instructions. Mammalian expression vectors coding for the mutated human IκBα-SuperRepressor (plasmid 15291), RelAS536E (plasmid 24156) and mammalian expression vectors pRK5-HA coding for ubiquitin wild type (WT) (plasmid 17608), ubiquitin K63 (plasmid 17606), EGFRL858R (plasmid 11012), EGFRExon19Del (plasmid 32062) were purchased from Addgene (Cambridge, MA, USA). The Rel-GFP construct was engineered with standard molecular cloning techniques using the pEGFP-N1 vector (Clontech). Plasmid coding for the NF-κB luciferase reporter (pGreenFire1-NFκB-Puro) was purchased from SBI (System Biosciences). The human IL6 expression construct was purchased from Genecopoeia.

shRNA constructs targeting human EGFR were purchased from Sigma-Aldrich. pBABE expression vectors for IL6, IKBSR, RelAS536E, EGFRL858R, and EGFRExon19Del were engineered using standard molecular biology techniques. 293-GPG viral packaging cells were transfected with pBABE (empty vector), pBABE-IL6, pBABE-IKBSR, pBABE-RelAS536E, pBABE-EGFRL858R, and pBABE-EGFRExon19Del constructs using Lipofectamine-2000 (Life Technologies, Pleasanton, CA) per manufacturer's instructions. Virus containing media was harvested three days post transfection and used to infect the indicated cell lines. Cells were incubated with virus containing media supplemented with 6 μg/ml of polybrene for 24 hours. Media was changed to standard cell growth media (RPMI-1640 + 10% fetal bovine serum and 100 U/ml penicillin G and 100 U/ml streptomycin SO_4) and cells were expanded for 48 hours, at which point puromycin (2 μg/ml) was added to the media and cells were allowed to grow for an additional 4 days. Cells that survived puromycin selection (stable cell lines) were used in all subsequent experiments.

To generate erlotinib or afatinib resistant cell lines, 1,000 HCC827 or H1975 cells were plated in a 96-well culture dish and exposed to continuous 1.0 micromolar erlotinib (for HCC827) or 1.0 micromolar afatinib (for H1975) in standard culture media over a period of 2-4 months with or without PBS-1086 (5.0 micromolar). Erlotinib/afatinib resistance was defined as the point at which cultures reached confluence in a 10 cm culture dish (~ 5 x 10^6 cells).

Animal Studies

Xenografts experiments were performed in female C.B. 17 Scid mice (C.B-Igh-1b/IcrTac-Prkdcscid) age 8-12 weeks. Tumors were allowed to grow until they reached a minimum volume of 200 mm^3 at which point mice were randomized to receive treatment

with vehicle (CMC, DMSO, Cremophor), erlotinib (12.5 mg/kg/d)(Bivona et al., 2011), PBS-1086 (7.5 mg/kg/d)(Fabre et al., 2012), or erlotinib + PBS-1086 by i.p. injection 5 days per week for 2 weeks. Tumor growth was assessed twice weekly by caliper measurements. A minimum of 10 tumors per treatment group were assessed for the duration of the study.

For transgenic experiments, the TetO-EGFRL858R (B6;SJL-Tg(tetO-Egfr*)2-9Jek/J) mice were bred to CC10-rtTA mice (B6.Cg-Tg(Scgb1a1-rtTA)1Jaw/J). The N1 generation was used for the experiments described. After 10 weeks of doxycycline exposure, mice were imaged by magnetic resonance (MR) using the 7T 300 MHz Horizontal Bore Varian MR System at the UCSF small imaging core to establish a baseline assessment of tumor volumes. Post-treatment MR imaging was performed and tumor volume pre-treatment was compared to tumor volumes obtained after 7 days of treatment using the ITK-Snap Version 2.2 imaging analysis software.

For PDX generation, a portion of the patient resected tumor was immediately placed in RPMI media and placed on wet ice. 1-2 mm^3 portions of tumor were then implanted onto the flanks of female C.B. 17 Scid mice (C.B-Igh-1b/IcrTac-Prkdcscid) age 8-12 weeks. Tumors were passaged to additional C.B. 17 Scid mice when they reached ~ 1000 mm^3 in size. PDX-tumor bearing mice were treated with vehicle (CMC, DMSO, Cremophor), erlotinib (25 mg/kg/d), PBS-1086 (7.5 mg/kg/d), or erlotinib + PBS-1086 by i.p. injection 5 days per week

Antibodies

For immunoblots, the following antibodies were used: pY1068-EGFR D7A5 (#3777), total EGFR D38B1 (#4267), EGFR E746-A750del D6B6 (Cell Signaling #2085) pS473-AKT D9E (#4060), total AKT (#9272), pT202/Y204-ERK1/2

D13.14.4E (#4370), total ERK1/2 (#3493), pY705-STAT3 D3A7 (#9145), total STAT3 123H6 (#9139), RelA (#8242) , Lamin B1 (#9087), HSP60 D307 (#4870), TRAF2 C192 (#4724), RIP1 D94C12 (#3493), IKKβ 2C8 (#2370), pS176/180-IKKα/β 16A6 (#2697), pS32-IκBα (#2370), Cleaved PARP 19F4 (#9546), and HA C29F4 (#3724), pTY1604-ALK (#3341) were purchased from Cell Signaling Technology. IκBα C-21 (sc-371), IKKγ 72C627 (sc-56919), GAPDH 6C5 (sc-32233) were purchased from Santa Cruz Biotechnology, Actin AC-74 from Sigma-Aldrich (#A2228) antibodies were purchased from Santa Cruz Biotechnology. HRP-conjugated anti-rabbit Ig (used at a 1:3000 dilution, Cell Signaling #7074), and HRP-conjugated anti-mouse IgG (used at a 1:3000 dilution, Cell Signaling #7076). Specific proteins were detected by using either ECL Prime (Amersham Biosciences, Sunnyvale, CA) or the Odyssey Li-Cor (Lincoln, NE) with the infrared dye (IR Dye 800, IR Dye 680)-conjugated secondary antibodies (1:20,000, Li-Cor). The QuantiGlo ELISA Kit (R&D Systems) was used per manufacturer's to quantify the amount of IL6 secreted into culture medium. Mouse monoclonal TRAF2 D-12 (sc-365287) and EGFR 528 (sc-120) antibodies for immunoprecipitation were purchased from Santa Cruz Biotechnology.

***In vivo* ubiquitination assay**

Plasmids coding for HA-ubiquitin (K63) were transfected in HCC827 cells. At 24 h after transfection, cells were treated for 30min with Erlotinib or Afatinib. Cells were harvested, lysed and boiled 5 min in 1% SDS (v/v) to remove all non-covalently associated proteins. Lysates were diluted 1:10 in RIPA buffer supplemented by 2 × protease inhibitor mixture (Roche). TRAF2 was immunoprecipitated using an anti-

TRAF2 antibody as described above. Proteins bound to the beads were then eluted in Laemmli buffer and subjected to immunoblot analysis. For the endogenous detection of the ubiquitinated TRAF2 the same procedure was followed without the transfection of HA-Ub_{K63} plasmid.

DNA Binding Assay

The ability of PBS-1086 to block the binding of activated transcription factors to their target DNA binding sites was evaluated using a DNA-binding ELISA (TransAM^{R} NF-κB, AP-1, and STAT Transcription Factor Assays, Active Motif). Nuclear extracts prepared from HeLa cells activated with TNFa (NF-κB family, p65/RelA), K-562 cells stimulated with TPA (AP-1 family), COS-7 cells treated with IFN-g (STAT1a), Hep G2 cells stimulated with IL-6 (STAT3), or Nb2 cells treated with prolactin (STAT5A and STAT5B) were added to 96-well microplates containing immobilized consensus binding site oligonucleotides. Transcription factor subunits bound to the DNA on the plate were detected with primary antibodies specific for each subunit followed by a HRP conjugated secondary antibody. The plates were treated with a colorimetric HRP substrate (TMB) and once the positive controls reached a dark blue color the reaction was stopped with acid yielding a yellow color. The absorbance at 450 nm was recorded as a measure of the amount of transcription factor bound to the DNA. Specificity of the assay was confirmed by the use of wild-type and mutant consensus oligonucleotide competitors.

To test the inhibitory activity of PBS-1086, stock solutions and intermediate dilutions of the compound were prepared in DMSO. Immediately before the assay, the compound was further diluted to the final test concentration (0.2 – 500 micromolar) in assay buffer and mixed with 1-3 mg of freshly thawed nuclear extracts for 30-120 minutes at room temperature prior to adding the treated extracts to the oligo-coated

microplates. Inhibition was determined from the quantity of transcription factor bound in the compound treated wells relative to the maximum quantity bound in the DMSO-only treated control wells (% inhibition = 1 − (PBS-1086 treated/DMSO treated) × 100). Sigmoidal dose-response curves were created by plotting the $\log_{10}$ (μM) concentration versus percent inhibition. DNA binding proteins studied included the NF-κB transcription factor (p65/RelA), the STAT family (STAT1a, STAT3, STAT5A, STAT5B), and the AP-1 family (c-fos, c-jun, FosB, Fra-1, JunB, JunD).

Immunohistochemistry

10 micron thick formalin-fixed paraffin embedded (FFPE) murine tissue sections were stained with the NF-κB p65 (RelA) rabbit polyclonal antibody (sc-109, Santa Cruz Biotechnology, 1:250 dilution), pY1068-EGFR D7A5 (#3777, Cell Signaling, 1:200 dilution), pT202/Y204-ERK1/2 D13.14.4E (#4370, Cell Signaling, 1:400 dilution), cleaved-caspase-3 (#9661, Cell Signaling Technologies, 1:200 dilution), the mouse monoclonal antibody Ki67 (KI67-MM1-L-CE, Leica Microsystems, 1:100 dilution), or the EGFR L858R Mutant Specific Rabbit monoclonal antibody (43B2, Cell Signaling Technologies #3197, 1:50 dilution) per manufacturer's instructions. Stained slides were digitized using the Aperio ScanScope CS Slide Scanner (Aperio Technologies) with a 40x objective. The proportion of cells exhibiting nuclear RelA staining, Ki67, or CC3 positivity was determined using the ScanScope default nuclear algorithm.

Mass Spectrometry

Frozen cell pellets were lysed in buffer containing 8M urea, 0.1M Tris pH 8.0, 150 mM NaCl, and a cocktail of protease inhibitors (Complete tablet, Roche). Protein concentration was measured by Bradford assay (QuickStart 1x Reagent, Bio-Rad). 10 mg

protein lysate from equal portions of light and heavy culture conditions were combined then subjected to reduction with 4 mM TCEP for 30 minutes at room temperature, alkylation with 10 mM iodoacetamide for 30 minutes and room temperature in the dark, and overnight digestion with 100 ug of trypsin (Promega) at room temperature. Treated lysates were subsequently desalted using SepPak C18 cartridges (Waters), lyophilized for two days and immunoprecipitated using an antibody specific for the K-GG motif characteristic of trypsinized, Ub-modified peptides (UbiScan, Cell Signaling Technology). Immunoprecipitates were then desalted using C18 STAGE tips (ThermoScientific), evaporated, and resuspend in 0.1% formic acid. Samples were analyzed on a Thermo Scientific LTQ Orbitrap Elite MS system equipped with an Easy nLC-1000 HPLC and autosampler. Samples were injected onto a C18 reverse phase capillary column (75 um inner diameter x 25 cm length, packed with 1.9 um C18 particles). Peptides were then separated by an organic gradient from 5% to 30% ACN in 0.1% formic acid over 120 minutes at a flow rate of 300 nl/min. The MS continuously collected spectra in a data-dependent fashion over the entire gradient. Variable modifications were allowed for methionine oxidation, lysine diglycine modification, and protein N-terminus acetylation. A fixed modification was indicated for cysteine carbamidomethylation. Full trypsin specificity was required. The first search was performed with a mass accuracy of +/- 20 parts per million and the main search was performed with a mass accuracy of +/- 6 parts per million. A maximum of 5 modifications were allowed per peptide. A maximum of 2 missed cleavages were allowed. The maximum charge allowed was 7+. Individual peptide mass tolerances were allowed. For MS/MS matching, a mass tolerance of 0.5 Da was allowed and the top 6 peaks per 100 Da were analyzed. MS/MS matching was allowed for higher charge states, water and ammonia loss events.

RNA Analysis

Total RNA was extracted from 11-18 cells transfected with expression constructs or treated with drug combinations as indicated using the RNeasy extraction kit (Qiagen). 2 mg of total RNA was used to generate libraries for deep sequencing using the Illumina Truseq (Illumina) sample preparation kit as previously described(Lin et al., 2014). To identify genes whose expression is regulated by NF-κB, we first identified genes with NF-κB ChIPseq and DNAse-I hypersensitive sites as defined by the ENCODE project(Bernstein et al., 2012) and that also contained a valid NF-κB binding site(Siggers et al., 2012). The set of genes within 15kb of these NF-κB binding sites was then intersected with the set of genes significantly upregulated in 11-18 cell lines expressing RelA-S536E when compared to parental 11-18's transfected with an empty vector; this set was intersected with the set of genes significantly downregulated in 11-18 cell lines expressing an IKBSR super-repressor compared to parental 11-18 cells transfected with an empty vector. This final set of 64 genes was clustered across each of our drug treatment conditions (11-18 + vehicle, 11-18 + erlotinib, 11-18 + PBS-1086, and 11-18 + erlotinib + PBS); a sub-cluster of 36 genes was identified from this clustering that were upregulated under erlotinib treatment and downregulated under combination treatment.

To validate gene expression changes observed in RNA-Seq analysis, we performed quantitative real-time PCR on total RNA isolated from lung cancer cells or tumor xenografts. RNA was extracted from cells or tumors using the RNeasy extraction kit, and cDNA synthesis was performed as described (Zhang et al., 2012). Samples were run in duplicate and GAPDH expression levels were used as an internal control for normalization of cDNA content. The QuantStudio 12K Flex V1.1.2 software was used to analyze Q-PCR data.

SUPPLEMENTAL REFERENCES

Bernstein, B.E., Birney, E., Dunham, I., Green, E.D., Gunter, C., and Snyder, M. (2012). An integrated encyclopedia of DNA elements in the human genome. Nature *489*, 57-74.

Bivona, T.G., Hieronymus, H., Parker, J., Chang, K., Taron, M., Rosell, R., Moonsamy, P., Dahlman, K., Miller, V.A., Costa, C.*, et al.* (2011). FAS and NF-kappaB signalling modulate dependence of lung cancers on mutant EGFR. Nature *471*, 523-526.

Fabre, C., Mimura, N., Bobb, K., Kong, S.Y., Gorgun, G., Cirstea, D., Hu, Y., Minami, J., Ohguchi, H., Zhang, J.*, et al.* (2012). Dual inhibition of canonical and non-canonical NF-kappaB pathways demonstrates significant anti-tumor activities in multiple myeloma. Clin Cancer Res.

Lin, L., Asthana, S., Chan, E., Bandyopadhyay, S., Martins, M.M., Olivas, V., Yan, J.J., Pham, L., Wang, M.M., Bollag, G.*, et al.* (2014). Mapping the molecular determinants of BRAF oncogene dependence in human lung cancer. Proc Natl Acad Sci U S A *111*, E748-757.

Siggers, T., Chang, A.B., Teixeira, A., Wong, D., Williams, K.J., Ahmed, B., Ragoussis, J., Udalova, I.A., Smale, S.T., and Bulyk, M.L. (2012). Principles of dimer-specific gene regulation revealed by a comprehensive characterization of NF-kappaB family DNA binding. Nature immunology *13*, 95-102.

Zhang, Z., Lee, J.C., Lin, L., Olivas, V., Au, V., Laframboise, T., Abdel-Rahman, M., Wang, X., Levine, A.D., Rho, J.K.*, et al.* (2012). Activation of the AXL kinase causes resistance to EGFR-targeted therapy in lung cancer. Nat Genet *44*, 852-860.